HHS Public Access

Author manuscript

J Bone Miner Res. Author manuscript; available in PMC 2017 January 17.

Published in final edited form as:

J Bone Miner Res. 2014 February ; 29(2): 361–369. doi:10.1002/jbmr.2049.

Neonatal Iron Deficiency Causes Abnormal Phosphate Metabolism by Elevating FGF23 in Normal and ADHR Mice

Erica L Clinkenbeard[1,*], **Emily G Farrow**[2,*], **Lelia J Summers**[1], **Taryn A Cass**[1], **Jessica L Roberts**[1], **Christine A Bayt**[1], **Tim Lahm**[3], **Marjorie Albrecht**[3], **Matthew R Allen**[4], **Munro Peacock**[5], and **Kenneth E White**[1]

[1]Department of Medical and Molecular Genetics, Indiana University School of Medicine, Indianapolis, IN, USA

[2]Clinical Center for Pediatric Genomic Medicine, Children's Mercy Hospitals Clinics, Kansas City, MO, USA

[3]Division of Pulmonary, Allergy, Critical Care and Occupational Medicine, Department of Medicine, Indiana University School of Medicine, Indianapolis, IN, USA

[4]Department of Anatomy and Cell Biology, Indiana University School of Medicine, Indianapolis, IN, USA

[5]Division of Endocrinology and Metabolism, Department of Medicine, Indiana University School of Medicine, Indianapolis, IN, USA

Abstract

Fibroblast growth factor 23 (FGF23) gain of function mutations can lead to autosomal dominant hypophosphatemic rickets (ADHR) disease onset at birth, or delayed onset following puberty or pregnancy. We previously demonstrated that the combination of iron deficiency and a knock-in R176Q FGF23 mutation in mature mice induced FGF23 expression and hypophosphatemia that paralleled the late-onset ADHR phenotype. Because anemia in pregnancy and in premature infants is common, the goal of this study was to test whether iron deficiency alters phosphate handling in neonatal life. Wild-type (WT) and ADHR female breeder mice were provided control or iron-deficient diets during pregnancy and nursing. Iron-deficient breeders were also made iron replete. Iron-deficient WT and ADHR pups were hypophosphatemic, with ADHR pups having significantly lower serum phosphate ($p < 0.01$) and widened growth plates. Both genotypes increased bone FGF23 mRNA (>50 fold; $p < 0.01$). WT and ADHR pups receiving low iron had elevated intact serum FGF23; ADHR mice were affected to a greater degree ($p < 0.01$). Iron-deficient mice also showed increased *Cyp24a1* and reduced *Cyp27b1*, and low serum 1,25-dihydroxyvitamin D (1,25D). Iron repletion normalized most abnormalities. Because iron

Address correspondence to: Kenneth E White, PhD, Department of Medical & Molecular Genetics, Indiana University School of Medicine, 975 West Walnut St., IB130, Indianapolis, IN 46202, USA. kenewhit@iupui.edu.

*ELC and EGF contributed equally to this work.

Disclosures

The other authors state that they have no conflicts of interest.

Authors' roles: EGF, ELC, TL, and KEW designed the research; ELC, EGF, LJS, TAC, JLR, TL, MA, MRA, CAB, MP, and KEW performed the research; TL and MA also provided reagents; ELC, EGF, TL, and KEW analyzed the data; and ELC, EGF, TL, MRA, MP, and KEW wrote the paper.

deficiency can induce tissue hypoxia, oxygen deprivation was tested as a regulator of FGF23, and was shown to stimulate FGF23 mRNA in vitro and serum C-terminal FGF23 in normal rats in vivo. These studies demonstrate that FGF23 is modulated by iron status in young WT and ADHR mice and that hypoxia independently controls FGF23 expression in situations of normal iron. Therefore, disturbed iron and oxygen metabolism in neonatal life may have important effects on skeletal function and structure through FGF23 activity on phosphate regulation.

Keywords

hypophosphatemia; iron; phosphate; kidney; bone; osteocyte

Introduction

Fibroblast growth factor-23 (FGF23) is a hormone produced in bone that controls renal phosphate reabsorption. The metabolic bone disease autosomal dominant hypophosphatemic rickets (ADHR; OMIM# 193100) is characterized by low serum phosphate concentrations as a result of decreased renal phosphate reabsorption, and by rickets/osteomalacia.[1] ADHR is caused by missense mutations that replace the arginine (R) residues at positions 176 or 179 with glutamine (Q) or tryptophan (W) (R176Q/W and R179Q/W)[2] within the FGF23 subtilisin-like proprotein convertase (SPC) site ($_{176}$RXXR$_{179}$/S$_{180}$).[2–5] These substitutions disrupt normal cleavage of the intact, bioactive form of the hormone. The ADHR phenotype parallels those of X-linked hypophosphatemic rickets (XLH; loss of function *PHEX* mutations), autosomal recessive hypophosphatemic rickets type 1 (ARHR1; loss of function *DMP1* mutations[6,7]) and ADHR type 2 (loss of function mutations in *ENPP1*[8,9]) and the acquired disorder, tumor-induced osteomalacia (TIO),[10] all of which have in common an elevation of plasma FGF23.

ADHR patients display incomplete penetrance and variable age of onset.[1] There are two subgroups of patients with ADHR: (1) those who present during childhood with hypophosphatemia, rickets, and lower extremity deformity; and (2) those who are unaffected early in life but then present clinically during adolescence or adulthood.[1] The early-onset patients have similar biochemical and skeletal profiles to those with XLH. But in contrast to XLH, the late ADHR onset patients can have waxing and waning of the hypophosphatemia that correlates with serum FGF23 concentrations.[11] Also, some patients treated early in life for hypophosphatemia have been documented to later lose the phosphate wasting defect.[1,11] FGF23 can be measured in plasma by two ELISAs: an “intact” assay that recognizes the bioactive molecule, and a C-terminal assay that recognizes intact FGF23 as well as proteolytic fragments C-terminal to the SPC RXXR site. Importantly, delayed-onset ADHR can coincide with puberty or pregnancy, common physiological situations of iron deficiency. We previously demonstrated that the combination of iron deficiency in the context of an FGF23 R176Q ADHR knock-in mutation in mice results in increased bone FGF23 mRNA and intact protein, causing an ADHR-like disease phenotype.[12] Of note, in the same study, mature wild-type (WT) mice were resistant to the effects of iron deficiency because of their ability to proteolytically cleave and inactivate FGF23 in the face of

increased production, as judged by elevated FGF23 mRNA with increased C-terminal FGF23 concentrations, but normal intact hormone.

In vivo, FGF23 acts in the kidney via its co-receptor αKlotho to reduce renal phosphate reabsorption through downregulation of the proximal tubule apical membrane sodium-phosphate cotransporter Npt2a, as well as suppression of the anabolic vitamin D 1α-hydroxylase (Cyp27b1) and increasing expression of the catabolic vitamin D 24-hydroxylase (Cyp24a1).[13,14] The net effect of these actions is to reduce both serum phosphate and 1,25-dihydroxyvitamin D (1,25D); parathyroid hormone (PTH) has the same effect on Npt2a, but converse effects on 1,25D metabolism. Normal iron and phosphate metabolism are critical for proper bone formation because iron overload and iron deficiency, as in heritable thalassemias, result in pathological changes in the skeleton.[15–18] Elevated C-terminal FGF23 has been associated with iron deficiency in cohorts of children, some with rickets.[19,20] However, whether there are functional and molecular consequences between iron and phosphate handling in normal neonates and in those with FGF23 ADHR mutations is unknown. Iron deficiency decreases oxygen delivery and causes tissue hypoxia; therefore, anemia and hypoxia induce similar regulatory responses, including stimulation of red cell production and the activation of survival genes such as erythropoietin (*EPO*) and vascular endothelial growth factor (*VEGF*), in a hypoxia-inducible factor transcription factor–dependent manner.[21] Because iron deficiency often occurs during pregnancy,[22] a goal of the present study was to test whether FGF23 can be induced in the neonate using an iron deficiency model based upon lack of maternal–neonatal iron transfer. In addition, we tested whether hypoxia independent of iron also controls FGF23 production.

Subjects and Methods

Animal studies

Animal studies were approved by the Institutional Animal Care and Use Committee (IACUC) for Indiana University, and complied with the NIH guidelines for the use of animals. ADHR R176Q-FGF23 mice are described[12] and were derived from standard gene targeting through embryonic stem cell (ES cell) transfer.

Rodent diets

Experimental diets were from Research Diets, Inc. (New Brunswick, NJ, USA). The “control-iron” diet was the AIN-76A base diet with the S10001 mineral mix containing iron at the standard concentration of 45 mg Fe/kg (carbonyl iron). The iron-deficient diet was the AIN-76A base diet and S10001 mineral mix with the iron removed (“low-iron” diet; ~0.1 parts per million [ppm] iron final). All diets contained customary 0.55% phosphate final, with low trace-element casein (Avicel PH101 cellulose). Iron repletion was carried out by first administering the low-iron diet at 14 days of pregnancy for 2 weeks, then providing the control-iron diet for 2 weeks. Diets and water were provided to the nursing mothers *ad libitum* throughout the experimental time frame.

In vivo hypoxia model

As described,[23] adult age-matched male (n = 5) Sprague-Dawley rats (250–275 g; Charles River, Wilmington, MA, USA) were exposed to hypobaric hypoxia (atmospheric pressure [P_{atm}] = 362 mmHg, equivalent to 10% fraction of inspired oxygen [FiO_2] at sea level, or an altitude of 5877 m) in a custom-made exposure chamber for a 2-week duration. Animals were allowed *ad libitum* access to food and water for the duration of the experimentation. Pressure and oxygen concentration in the chamber were continuously monitored by adequately calibrated sensors. The chamber was opened daily for 30 minutes for change of bedding and water. Age-matched controls were housed at ambient barometric pressure (~760 mmHg). All animals were maintained on a 12-hour:12-hour light:dark cycle and received care in compliance with the Guide for the Care and Use of Laboratory Animals. At the end of hypoxia exposure, rats were killed immediately upon removal from the chamber by isoflurane overdose and exsanguination. Blood was drawn by right ventricular puncture. Samples were centrifuged for procurement of plasma, which was then snap frozen in liquid nitrogen.

Serum biochemistries

Blood samples were collected from mice at the time of death by cardiac puncture, or by tail bleed according to approved protocols. Routine serum biochemistries including calcium (Ca), phosphate (Pi), alkaline phosphatase (AP), creatinine (Cr), and total serum iron were measured using an automated COBAS MIRA Plus Chemistry Analyzer (Roche Diagnostics, Indianapolis, IN, USA). Serum 1,25D was measured using an enzyme immunoassay (EIA) (Immunodiagnostic Systems Inc., Scottsdale, AZ, USA) according to the manufacturer's instructions. Serum intact FGF23 concentrations were assessed using a commercial ELISA (Kainos Laboratories International, Tokyo, Japan). FGF23 was also measured using a rodent-specific C-terminal FGF23 ELISA that recognizes full-length FGF23 and peptides 3′ (C-terminal) to the SPC site, according to the manufacturer's specifications (Immutopics International, San Clemente, CA, USA).

Histomorphometry

Distal femurs collected at the time of death were embedded in methyl methacrylate, and midsagittal (4-μm) sections of cancellous bone from the distal femur were cut using a microtome (2050 Supercut; Reichert-Jung, Depew, NY, USA). The sections were stained with McNeal/Tetrachrome stain according to established protocols, and were examined blinded to mouse diet and genotype. Histomorphometric measures of growth plate thickness were obtained at the central region of the image where the growth plate was perpendicular to the place of section using a semiautomatic analysis system (Bioquant OSTEO; Bioquant Image Analysis Co., Nashville, TN, USA) attached to a Nikon microscope.

RNA preparation and quantitative PCR

Kidney and bone were harvested and homogenized in 1 mL of TRIzol reagent (Invitrogen, Inc., Carlsbad, CA, USA) according to the manufacturer's protocol using a TissueTearor rotor-stator (Biospec Products, Inc., Bartlesville, OK, USA). UMR-106 total cell RNA was collected with the RNeasy Kit (Qiagen, Inc., Gaithersburg, MD, USA) according to the

manufacturer's directions. RNA samples were tested with primers specific for mouse vitamin D 24-hydroxylase (*Cyp24a1*), vitamin D 1-α-hydroxylase (*Cyp27b1*), *FGF23*, *EPO*, and transferrin receptor-1 (*TfRc1*) and for rat *FGF23*; rodent β-actin was used as an internal control. quantitative PCR (qPCR) primers and probes were either purchased as preoptimized reagents (Life Technologies, Rockville, MD, USA), or designed in-house; sequences are available upon request.

The TaqMan One-Step RT-PCR kit was used to perform qPCR. PCR conditions for all experiments were as follows: 30 minutes at 48°C, 10 minutes at 95°C, followed by 40 cycles of 15 seconds at 95°C and 1 minute at 60°C. The data was collected and analyzed by the 7500 Real Time PCR system and software (Applied Biosystems, Foster City, CA, USA). The expression levels of mRNAs were calculated relative to WT mice receiving the control diet. All primer sets were tested for specific amplification of mRNA by parallel analyses of controls that included omitting reverse transcriptase (RT) or template, and resulted in no fluorescent signal detection. Each RNA sample was analyzed in at least triplicate, and each in vitro experiment was performed independently at least three times. The delta-delta comparative cycle threshold ($2^{-\Delta\Delta Ct}$) method described by Livak and Schmittgen[24] was used to analyze the data.

Cell culture

UMR-106 cells (ATCC) were cultured in D-MEM/F-12 (Invitrogen, Thermo-Fisher Scientific, Waltham, MA, USA) supplemented with 10% fetal bovine serum (FBS; Hyclone), 1 mM sodium pyruvate, 25 mM L-glutamine, and 25 mM penicillin-streptomycin (Sigma-Aldrich, St. Louis, MO, USA) at 37°C and 5% CO_2. Cells were cultured under normoxia or the same conditions but at 0.5 ATM (10% O_2).

Immunoblots

UMR-106 cells were lysed with 100 μL 1× Lysis buffer (Cell Signaling Technologies, Inc., Danvers, MA, USA) with 1 μg/mL 4-(2-aminoethyl) benzenesulfonyl fluoride hydrochloride (AEBSF) protease inhibitor (Sigma-Aldrich, Inc.). Cell lysate protein concentrations were determined with the Better Bradford Kit (Thermo-Fisher Scientific) according to the manufacturer's instructions. Western blot analysis was performed with 30 μg UMR-106 cellular lysates. The blots were incubated with primary antibody to hypoxia-inducible factor 1-alpha (HIF1α) (NB100–449; Novus Biologicals, Littleton, CO, USA) at 1:1000, then incubated with secondary antibody at 1:3000 (anti-rabbit–horseradish peroxidase [HRP]; BioRad, Inc., Hercules, CA, USA). Blots were stripped using SDS-glycine and reprobed with 1:10,000 anti-β-actin-HRP (A3854; Sigma-Aldrich). Detection was performed using the ECL Prime Western Blotting Detection Reagents (Amersham-GE Healthcare, Pittsburgh, PA, USA) and XOMAT film (Eastman-Kodak Co., Rochester, NY, USA).

Statistical analysis

Significance between groups was assessed using ANOVA analysis with a Tukey honestly significant difference (HSD) post hoc test. Differences between low-iron and replete samples and RNA expression in UMR-106 cells were assessed with Student's *t* test. Significance for all tests was set at $p < 0.05$ and data are presented as means ± SEM.

Results

Iron deficiency and early-onset hypophosphatemia

Whether maternal iron deficiency during pregnancy (typically found in the third trimester) and nursing can alter the molecular mechanisms underlying control of FGF23 is not known. To address this question, female mouse breeders were provided diets with normal ("control-iron"; 45 mg/kg iron), or "low-iron" (0% added iron) from day 14 of pregnancy through weaning (21 days after birth), and WT and heterozygous ADHR pups were examined. This dietary protocol resulted in iron deficiency as determined by elevated renal EPO ($p < 0.01$; Fig. 1*A*) and transferrin receptor type 1 (TfRc1; $p < 0.01$, Fig. 1*B*) mRNA expression in both the ADHR and WT pups receiving low iron.

The effects of maternal iron deficiency on serum biochemistries related to phosphate homeostasis were next tested. The ADHR and WT mice on the control diet had similar serum biochemistries. Iron-deficient WT pups had modest hypophosphatemia compared to the control diet pups ($p < 0.01$), whereas the ADHR mice had a more dramatic reduction in serum phosphate compared to both the control diet ADHR mice and to WT low-iron mice ($p < 0.01$ versus ADHR control diet and WT low-iron diet; Fig. 2*A*). Serum 1,25D was significantly reduced in both the iron-deficient WT and ADHR mice compared to mice receiving the control diet ($p < 0.01$; Fig. 2*B*). Serum calcium in the WT low-iron group and alkaline phosphatase in the ADHR control group were slightly elevated ($p < 0.01$, $p < 0.05$, respectively; data not shown), whereas creatinine levels remained unchanged between groups (data not shown).

Control of circulating FGF23

To test the regulation of circulating FGF23 following iron deficiency in the ADHR mice in vivo, two serum assays were employed: an intact FGF23 ELISA that recognizes whole-molecule FGF23, as well as a C-terminal FGF23 ELISA that measures the intact protein and in addition the FGF23 proteolytic fragments C-terminal to the FGF23 $_{176}$RXXR$_{179}$/S$_{180}$ SPC site. In the WT pups with iron deficiency, intact FGF23 was elevated versus control-diet pups ($p < 0.01$; Fig. 2*C*). Intact FGF23 was also increased in the ADHR iron-deficient mice versus ADHR control diet mice and WT low-iron diet mice ($p < 0.01$ versus ADHR control; $p < 0.05$ versus WT low-iron; Fig. 2*C*). The iron-deficient WT and ADHR pups had highly elevated serum C-terminal FGF23 concentrations and, similar to the intact FGF23, this was also significantly increased in ADHR low-iron mice versus the WT iron-deficient group ($p < 0.01$ versus ADHR control diet and WT low iron; Fig. 2*D*).

Analysis of kidney gene expression showed reduced renal *Cyp27b1* and elevated *Cyp24a1* mRNAs in the iron-deficient WT and ADHR pups as compared to the pups receiving the control diet (Fig. 3*A*, *B*), with a significantly greater degree of changes present in the ADHR mice. To test the mechanisms underlying the increased circulating FGF23 protein, RNA was isolated from femur/tibia following low-iron or control diet, and FGF23 mRNA expression was tested by qPCR. With low-iron treatment, the WT and ADHR mice had similar increases in FGF23 mRNA (>50-fold) compared to pups receiving the control diet ($p < 0.01$ for ADHR and WT low-iron versus control; Fig. 3*C*).

Fixed sections of distal femur from pups receiving each diet were stained and assessed by histomorphometry. Analyses revealed widened growth plates due to expanded zone of calcification in the ADHR low-iron group (Fig. 4*A*) that was significantly different from the WT control, WT low-iron, and ADHR control diet groups (Fig. 4*B*; $p < 0.01$ to 0.05).

Effects of iron repletion

To test whether the increased FGF23 and hypophosphatemia induced by iron deficiency could be abolished during the neonatal period, breeders were placed on the low-iron diet on day 14 of pregnancy as usual, but after 2 weeks (1 week in utero and 1 week after birth), the mothers were switched to the control iron diet for the final 2 nursing weeks. This regimen resulted in serum phosphate at 4 weeks (2 weeks iron-replete) that was normalized versus ADHR mice that were continuously provided the low-iron diet (Table 1). Intact and C-terminal FGF23 concentrations were similar to those of ADHR mice continuously receiving control iron diet (Table 1). The replete group was also normal for bone FGF23 and kidney *Cyp24a1* mRNAs; however, *Cyp27b1* mRNA remained suppressed (Table 1).

Hypoxia and FGF23 expression

Systemic iron deficiency and oxygen deficiency control some similar sets of compensatory genes, such as *EPO* and *VEGF*. We previously demonstrated that treatment with the iron chelator deferoxamine (DFO) resulted in elevated FGF23 under normoxia in UMR-106 cells.[12] Thus we next tested the hypothesis that hypoxia could induce FGF23 expression independently from changes in iron. To study the effects of oxygen tension, UMR-106 cells were grown in 0.5 ATM (10% O_2) or normoxia (21%) for 24 or 48 hours. With a decrease in oxygen tension but constant cell media iron concentrations, FGF23 mRNA was significantly elevated at 24 hours, and approached normal by 48 hours (Fig. 5*A*). In parallel, immunoblots from UMR-106 cell lysates showed that HIF1α protein was modestly elevated at 4 hours, consistent with a hypoxic response, then reduced by 24 and 48 hours (Fig. 5*A*; inset), which paralleled the FGF23 mRNA expression time course. To extend this to in vivo situations, Sprague-Dawley rats ($n = 5$/group) were housed in a hypobaric atmosphere for 2 weeks at 362 mmHg (equivalent to 10% FiO_2) or kept under normoxic conditions. As demonstrated,[23] when compared to normoxic control animals, hypoxia caused robust erythrocytosis (hematocrit: 62.5% ± 1.0% versus 38.2% ± 1.2%; $p < 0.001$), pulmonary hypertension (right ventricular systolic pressure: 57.3 ± 2.9 mmHg versus 31.1 ± 1.9 mmHg; $p < 0.001$), and right ventricular hypertrophy (right ventricular weight/weight of left ventricle plus septum [RV/LV + S]: 52.0% ± 1.5% versus 27.3% ± 1.0%; $p < 0.001$). Collectively, these findings confirm in vivo hypobaric hypoxia. Interestingly, parallel serum FGF23 measurements demonstrated that C-terminal FGF23 was significantly elevated (>6-fold; Fig. 5*B*) in the hypoxic group, whereas intact FGF23 was not different between the hypoxic and normoxic group (Fig. 4*B*). Serum phosphate (normoxic: 6.9 ± 0.4 mg/dL; hypoxic: 7.5 ± 0.8 mg/dL) and total iron concentrations (normoxic: 277.2 ± 37.2 mg/dL; hypoxic: 281.3 ± 37.2 mg/dL) were not different between treatments. These results support the concept that hypoxia may control FGF23 independently of iron, and that the processing of FGF23 into C-terminal fragments occurs in low oxygen and in rodents made iron-deficient through diet, in order to maintain normal serum phosphate concentrations.[12]

Discussion

Herein, we found that iron deficiency anemia in young mice significantly increased FGF23 production and resulted in hypophosphatemia and altered 1,25D metabolism. In this regard, provision of an iron-deficient diet to breeder mothers during the last week of pregnancy and while nursing, mimicking the third human trimester when iron deficiency is common and results in elevated tissue production of EPO and TFRc1,[25,26] reliable physiologic markers of iron deficiency. With this regimen, intact and C-terminal FGF23 were also elevated in both WT and ADHR mice. The FGF23 increases were significantly greater in the ADHR mice, and led to greater reductions in serum phosphate and 1,25D, suggesting that the increase in FGF23 in the ADHR mice was biologically active. Although the iron-deficiency–dependent increases in FGF23 mRNA were similar in WT and ADHR mice, it is likely that the WT form of FGF23 was more amenable to SPC cleavage, consistent with previous in vitro results examining recombinant FGF23 protein.[3,4] These effects were partially mimicked by anoxia in rats and reversed by iron repletion in mice.

Importantly, unlike the situation in mature mice,[12] WT neonatal mice were unable to fully counteract the increase in FGF23 mRNA through proteolysis of the translated hormone, leading to elevated intact FGF23 and decreased serum phosphate and 1,25D levels above those in WT mice receiving the control diet. This FGF23 response to iron deficiency in WT healthy mice may point to an important role of iron in the manifestation of rickets in both neonatal and postnatal periods of life. In the premature infant and in the case of neonatal vitamin D deficiency, rickets is often attributable to the inability to supply sufficient phosphate via the diet, resulting in hypophosphatemic rickets.[27] Our data suggest that an accompanying iron deficiency or anoxic state is likely to aggravate the onset and severity of the rickets, and suggest that measures of iron status are likely to be useful in diagnosing, managing, and treating rickets in children.

The reason for the biological intersection of iron and phosphate homeostasis through FGF23, as well as the need and mechanisms for complete resistance to iron deficiency–dependent increases in FGF23 in mature animals is not completely clear, and is likely complex. We demonstrated that providing iron to WT and ADHR mice that had been deprived of iron resulted in pups with abnormal FGF23 and phosphate handling. These findings support the concept that balance of iron and phosphate during pregnancy and nursing is critical during differentiation and growth of the skeleton. Indeed, the increase in WT FGF23 had marked biological effects on renal 1,25D metabolic enzymes, with increased Cyp24a1 and reduced Cyp27b1 mRNAs. Of note, although intact FGF23 was not different between the ADHR mice receiving the control diet and those receiving the iron replacement diet, the Cyp27b1 remained abnormal, indicating that there is a lag time between restoration of FGF23 and the return of normal phosphate homeostasis. Our work demonstrated that the stimulatory effects of iron deprivation are much stronger biological influences on FGF23 production than the known in vivo suppressive effects of hypophosphatemia previously derived through diet[28,29] or in other genetic models such as the vitamin D receptor (VDR)-null mouse.[30] The alterations in the control of FGF23 under conditions of iron deficiency could also speculatively have implications beyond rare heritable disorders. In pediatric patients with stage 3 chronic kidney disease–mineral and bone disorder (CKD-MBD),

approximately 65% are anemic, which rises to over 90% by stage 4/5[31]; and importantly, iron deficiency is the most common mineral deficiency in children worldwide.[32] Whether FGF23 is processed differently in childhood than in adult CKD-MBD, and whether the crossover control of FGF23 and iron/hypoxia in the young has metabolic effects on bone growth and development remains to be determined.

Iron deficiency anemia results in reduced oxygen delivery to tissues and in hypoxic states, and overlapping compensatory mechanisms to reductions in iron are activated. The differential effects of hypoxia on circulating forms of FGF23 in mature normal rats (normal intact but elevated C-terminal FGF23) is similar to the effects on FGF23 processing caused by iron deficiency in mature WT mice.[12] In agreement with the in vivo studies, hypoxia increased FGF23 mRNA in UMR-106 cells, and FGF23 expression correlated with the cellular stabilization of HIF1α. We have also demonstrated that HIF activity could also be induced in parallel with FGF23 using the iron chelator DFO.[12] Previous studies using UMR-106 cells demonstrated that other osteoblast/osteocyte genes can be controlled by hypoxia, including SOST, which is significantly reduced in parallel with increased expression and nuclear localization of activated β-catenin.[33] In agreement, studies support that DMP1, MEPE, Connexin-43, and FGF23 may be controlled by hypoxia in MC3T3 cells and primary cultures of osteoblasts.[34] Potentially, the interconnected control of these genes functions as a portion of a tissue and cell maturation program that may be required to balance mineralization through systemic phosphate control (FGF23), local osteoblast function (SOST, Connexin-43), and matrix deposition (DMP1, MEPE). Further, it is most likely that the marked hypophosphatemia in the ADHR low-iron diet animals resulted in the expanded growth plate zone of calcification typical of rickets. Because HIF1α is known to control important regulators of vasculogenesis, parallel control of systemic FGF23 could potentially act to optimize blood phosphate, thus mineralizing bone as vascularization occurs. By extension, skeletal fracture repair initially occurs in a hypoxic environment as blood vessels are broken, and these coordinated changes in gene expression and cell differentiation could act to maximize the skeletal healing process. Indeed, FGF23 mRNA has been found to be highly expressed in cells along fracture callus.[35]

In summary, our findings demonstrate that FGF23 is elevated during iron deficiency through maternal-neonatal transfer. In the presence of an ADHR R176Q-FGF23 allele in mice, this biological situation leads to more severe hypophosphatemia compared to mice expressing the WT FGF23 alleles. Hypoxia with normal iron also increased FGF23 mRNA in vitro and had differential effects on FGF23 protein in vivo. Collectively, these results provide a link between phosphate and iron metabolism early in life and may reveal new roles for FGF23 in normal growth.

Acknowledgments

This work was supported by NIH grants DK063934, DK095784, and AR059278, a Genzyme GRIP award, the Indiana Genomics Initiative (INGEN) of Indiana University, supported in part by the Lilly Endowment, Inc. (to KEW); NIH-UL1RR025761 (to MP); NIH grant AR062002 (to MRA); and an American Thoracic Society/ Pulmonary Hypertension Association/Pfizer Fellowship in Pulmonary Arterial Hypertension Research and an IUPUI Research Support Funds Grant (to TL). EGF was supported through a National Kidney Foundation postdoctoral fellowship.

KEW receives royalties from Kyowa Hakko Kirin Co. Ltd., and MP is involved in a clinical trial with Kyowa Hakko Kirin Co. Ltd.

References

1. Econs MJ, McEnery PT. Autosomal dominant hypophosphatemic rickets/osteomalacia: clinical characterization of a novel renal phosphate-wasting disorder. J Clin Endocrinol Metab. 1997; 82(2): 674–681. [PubMed: 9024275]
2. ADHR-Consortium. Autosomal dominant hypophosphataemic rickets is associated with mutations in FGF23. Nat Genet. 2000; 26(3):345–348. [PubMed: 11062477]
3. White KE, Carn G, Lorenz-Depiereux B, Benet-Pages A, Strom TM, Econs MJ. Autosomal-dominant hypophosphatemic rickets (ADHR) mutations stabilize FGF-23. Kidney Int. 2001; 60(6): 2079–2086. [PubMed: 11737582]
4. Shimada T, Muto T, Urakawa I, et al. Mutant FGF-23 responsible for autosomal dominant hypophosphatemic rickets is resistant to proteolytic cleavage and causes hypophosphatemia in vivo. Endocrinology. 2002; 143(8):3179–3182. [PubMed: 12130585]
5. Gribaa M, Younes M, Bouyacoub Y, et al. An autosomal dominant hypophosphatemic rickets phenotype in a Tunisian family caused by a new FGF23 missense mutation. J Bone Miner Metab. 2010; 28(1):111–115. [PubMed: 19655082]
6. Feng JQ, Ward LM, Liu S, et al. Loss of DMP1 causes rickets and osteomalacia and identifies a role for osteocytes in mineral metabolism. Nat Genet. 2006; 38(11):1310–1315. [PubMed: 17033621]
7. Lorenz-Depiereux B, Bastepe M, Benet-Pages A, et al. DMP1 mutations in autosomal recessive hypophosphatemia implicate a bone matrix protein in the regulation of phosphate homeostasis. Nat Genet. 2006; 38(11):1248–1250. [PubMed: 17033625]
8. Lorenz-Depiereux B, Schnabel D, Tiosano D, Hausler G, Strom TM. Loss-of-function ENPP1 mutations cause both generalized arterial calcification of infancy and autosomal-recessive hypophosphatemic rickets. Am J Hum Genet. 2010; 86(2):267–272. [PubMed: 20137773]
9. Saito T, Shimizu Y, Hori M, et al. A patient with hypophosphatemic rickets and ossification of posterior longitudinal ligament caused by a novel homozygous mutation in ENPP1 gene. Bone. 2011; 49(4):913–916. [PubMed: 21745613]
10. Tenenhouse, HS.; Econs, MJ. Mendelian hypophosphatemias. In: Valle, D., editor. The metabolic and molecular bases of inherited disease. New York: McGraw-Hill; 2001. p. 1-9.
11. Imel EA, Hui SL, Econs MJ. FGF23 concentrations vary with disease status in autosomal dominant hypophosphatemic rickets. J Bone Miner Res. 2007; 22(4):520–526. [PubMed: 17227222]
12. Farrow EG, Yu X, Summers LJ, et al. Iron deficiency drives an autosomal dominant hypophosphatemic rickets (ADHR) phenotype in fibroblast growth factor-23 (Fgf23) knock-in mice. Proc Natl Acad Sci U S.A. 2011; 108(46):E1146–E1155. [PubMed: 22006328]
13. Shimada T, Mizutani S, Muto T, et al. Cloning, characterization of FGF23 as a causative factor of tumor-induced osteomalacia. Proc Natl Acad Sci U S.A. 2001; 98(11):6500–6505. [PubMed: 11344269]
14. Larsson T, Marsell R, Schipani E, et al. Transgenic mice expressing fibroblast growth factor 23 under the control of the alpha1(I) collagen promoter exhibit growth retardation, osteomalacia, and disturbed phosphate homeostasis. Endocrinology. 2004; 145(7):3087–3094. [PubMed: 14988389]
15. Haidar R, Musallam KM, Taher AT. Bone disease and skeletal complications in patients with beta thalassemia major. Bone. 2011; 48(3):425–432. [PubMed: 21035575]
16. Diaz-Castro J, Lopez-Frias MR, Campos MS, et al. Severe nutritional iron-deficiency anaemia has a negative effect on some bone turnover biomarkers in rats. Eur J Nutr. 2012; 51(2):241–247. [PubMed: 21647667]
17. Terpos E, Voskaridou E. Treatment options for thalassemia patients with osteoporosis. Ann N Y Acad Sci. 2010; 1202:237–243. [PubMed: 20712799]
18. Voskaridou E, Stoupa E, Antoniadou L, et al. Osteoporosis and osteosclerosis in sickle cell/beta-thalassemia: the role of the RANKL/osteoprotegerin axis. Haematologica. 2006; 91(6):813–816. [PubMed: 16704959]

19. Braithwaite V, Jarjou LM, Goldberg GR, Jones H, Pettifor JM, Prentice A. Follow-up study of Gambian children with rickets-like bone deformities and elevated plasma FGF23: possible aetiological factors. Bone. 2012; 50(1):218–225. [PubMed: 22023931]
20. Braithwaite V, Jarjou LM, Goldberg GR, Prentice A. Iron status and fibroblast growth factor-23 in Gambian children. Bone. 2012; 50(6):1351–1356. [PubMed: 22465847]
21. Chepelev NL, Willmore WG. Regulation of iron pathways in response to hypoxia. Free Radic Biol Med. 2011; 50(6):645–666. [PubMed: 21185934]
22. Breymann C, Honegger C, Holzgreve W, Surbek D. Diagnosis and treatment of iron-deficiency anaemia during pregnancy and postpartum. Arch Gynecol Obstet. 2010; 282(5):577–580. [PubMed: 20577752]
23. Lahm T, Albrecht M, Fisher AJ, et al. 17beta-Estradiol attenuates hypoxic pulmonary hypertension via estrogen receptor-mediated effects. Am J Respir Crit Care Med. 2012; 185(9):965–980. [PubMed: 22383500]
24. Livak KJ, Schmittgen TD. Analysis of relative gene expression data using real-time quantitative PCR and the 2(−Delta Delta C(T)) method. Methods. 2001; 25(4):402–408. [PubMed: 11846609]
25. Wang GL, Semenza GL. Desferrioxamine induces erythropoietin gene expression and hypoxia-inducible factor 1 DNA-binding activity: implications for models of hypoxia signal transduction. Blood. 1993; 82(12):3610–3615. [PubMed: 8260699]
26. Bianchi L, Tacchini L, Cairo G. HIF-1-mediated activation of transferrin receptor gene transcription by iron chelation. Nucleic Acids Res. 1999; 27(21):4223–4227. [PubMed: 10518614]
27. Abrams SA. In utero physiology: role in nutrient delivery and fetal development for calcium, phosphorus, and vitamin D. Am J Clin Nutr. 2007; 85(2):604S–607S. [PubMed: 17284763]
28. Antoniucci DM, Yamashita T, Portale AA. Dietary phosphorus regulates serum fibroblast growth factor-23 concentrations in healthy men. J Clin Endocrinol Metab. 2006; 91(8):3144–3149. [PubMed: 16735491]
29. Burnett SM, Gunawardene SC, Bringhurst FR, Juppner H, Lee H, Finkelstein JS. Regulation of C-terminal and intact FGF-23 by dietary phosphate in men and women. J Bone Miner Res. 2006; 21(8):1187–1196. [PubMed: 16869716]
30. Yu X, Sabbagh Y, Davis SI, Demay MB, White KE. Genetic dissection of phosphate- and vitamin D-mediated regulation of circulating Fgf23 concentrations. Bone. 2005; 36(6):971–977. [PubMed: 15869926]
31. Wong H, Mylrea K, Feber J, Drukker A, Filler G. Prevalence of complications in children with chronic kidney disease according to KDOQI. Kidney Int. 2006; 70(3):585–590. [PubMed: 16788689]
32. Miller JL. Iron deficiency anemia: a common and curable disease. Cold Spring Harb Perspect Med. 2013 Jul 1.3(7)
33. Genetos DC, Toupadakis CA, Raheja LF, et al. Hypoxia decreases sclerostin expression and increases Wnt signaling in osteoblasts. J Cell Biochem. 2010; 110(2):457–467. [PubMed: 20336693]
34. Hirao M, Hashimoto J, Yamasaki N, et al. Oxygen tension is an important mediator of the transformation of osteoblasts to osteocytes. J Bone Miner Metab. 2007; 25(5):266–276. [PubMed: 17704991]
35. Riminucci M, Collins MT, Fedarko NS, et al. FGF-23 in fibrous dysplasia of bone and its relationship to renal phosphate wasting. J Clin Invest. 2003; 112(5):683–692. [PubMed: 12952917]

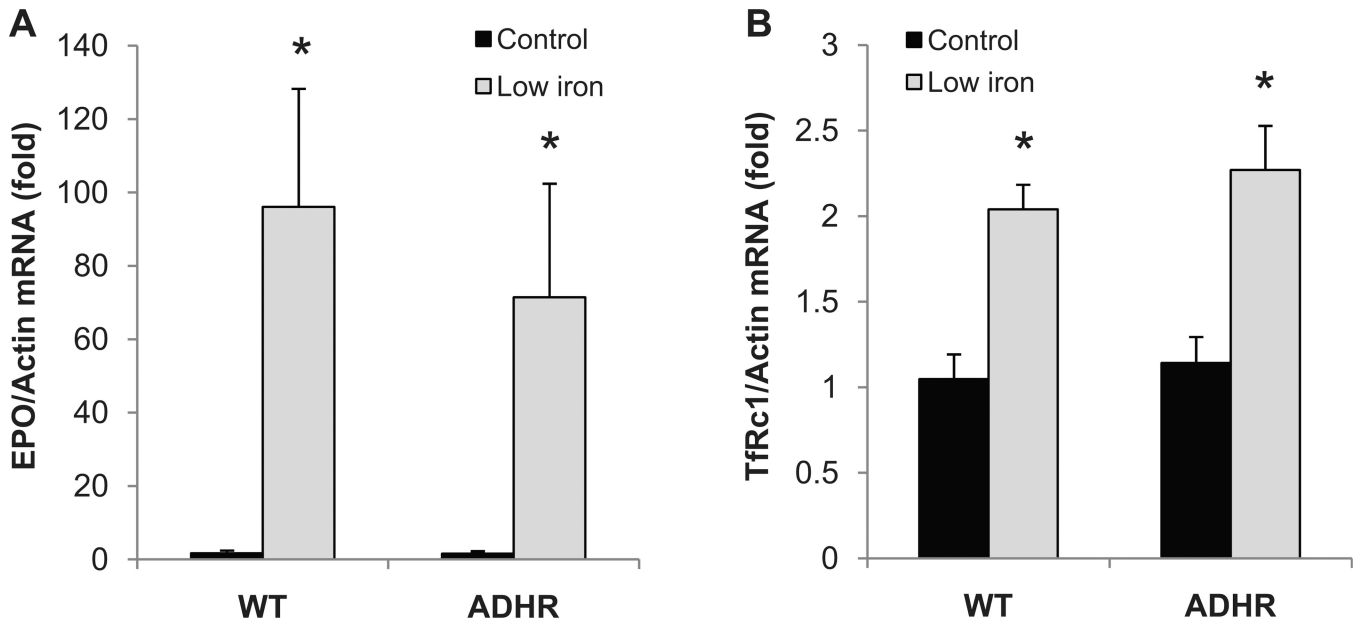

Fig. 1.

Response of EPO and *TfRc1* to iron deficiency. (*A*) Kidney erythropoietin (EPO) mRNA was significantly elevated in ADHR and WT pups ($n \geq 9$/group) from mothers receiving a low-iron diet versus pups from mothers receiving a control iron diet. (*B*) Kidney *TfRc1* was also significantly increased in the low-iron diet mice (*$p < 0.01$ versus either genotype receiving control iron diet).

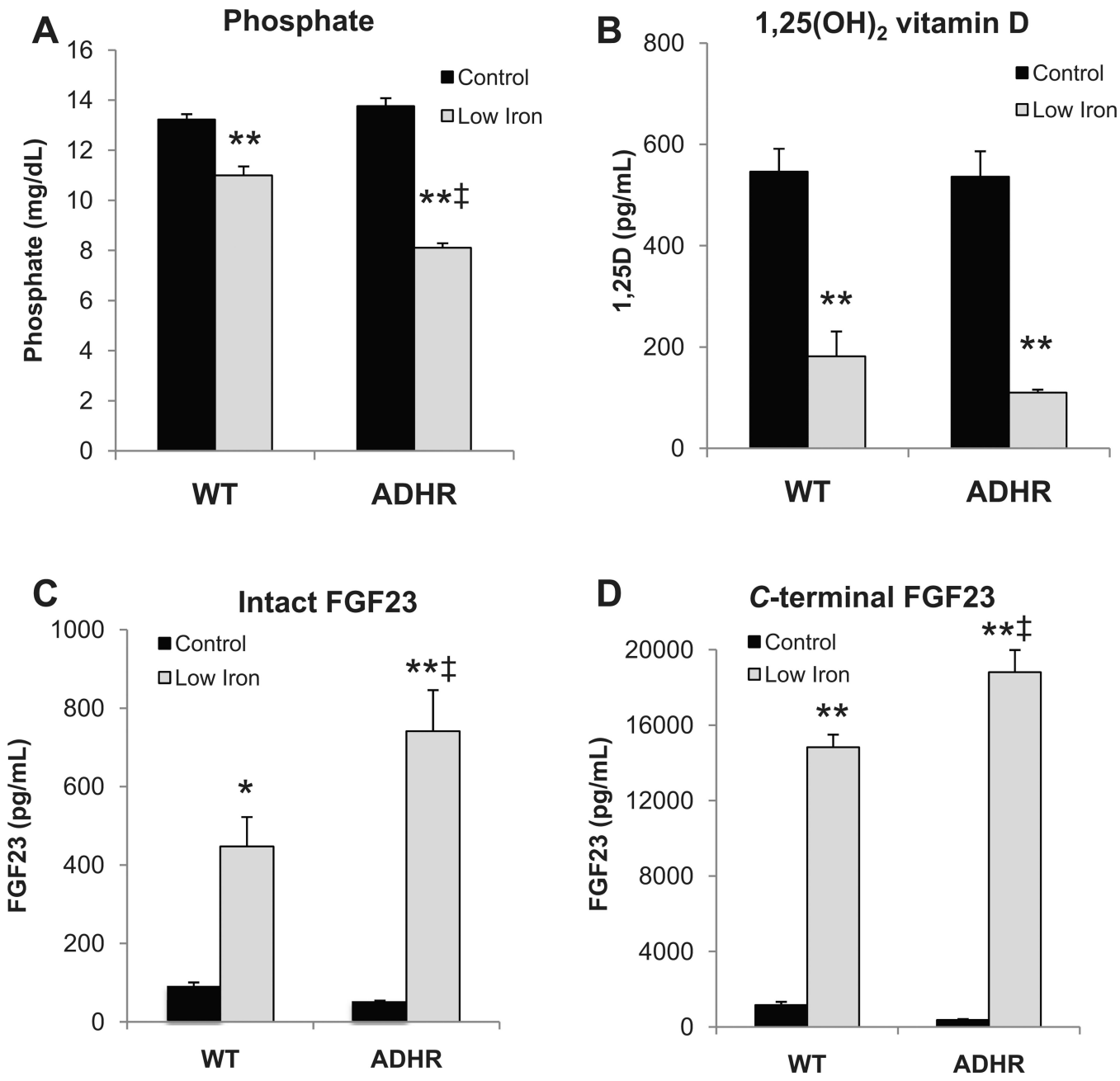

Fig. 2.

Biochemical variables. (*A*) Serum phosphate was reduced in both ADHR and WT mice ($n \geq 19$/group) receiving the iron-deficient diet (*$p < 0.01$ versus control diet; ‡$p < 0.01$ versus low-iron WT cohort). (*B*) Serum 1,25D was decreased in the mice ($n = 6–9$/group) receiving the low-iron diet (*$p < 0.01$ versus like genotype control iron diet; ‡$p < 0.05$ versus WT receiving low iron). (*C*) Intact and (*D*) C-terminal FGF23 were increased in ADHR and WT mice ($n \geq 20$/group) receiving the low-iron diet when compared to like genotype receiving the control iron diet (*$p < 0.05$; **$p < 0.01$), and ADHR mice receiving low iron were significantly elevated compared to WT mice provided low iron (‡$p < 0.01$).

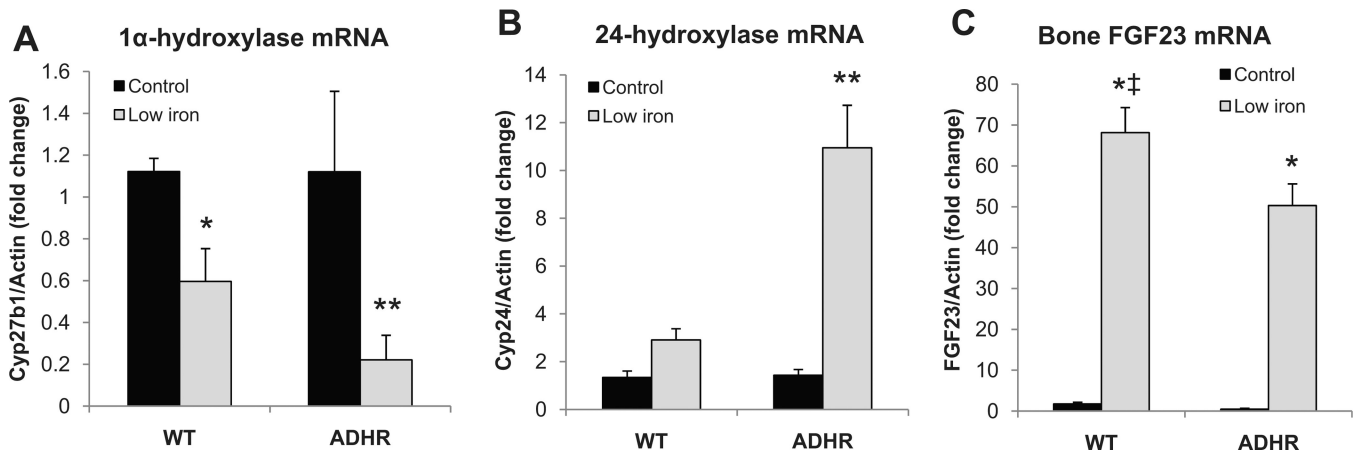

Fig. 3.

Renal and bone mRNA changes in iron-deficient pups. (*A*) Renal 1-α-hydroxylase (*Cyp27b1*) mRNA was reduced in both WT and ADHR mice receiving low iron; and (*B*) renal 24-hydroxylase (*Cyp24a1*) mRNA was elevated in ADHR neonates receiving low iron (*$p < 0.05$; **$p < 0.01$). (*C*) Bone FGF23 mRNA was significantly increased with low-iron diet regimen (*$p < 0.01$ versus same genotype control diet; $^{‡}p < 0.05$ versus low iron ADHR group; $n \geq 9$/group).

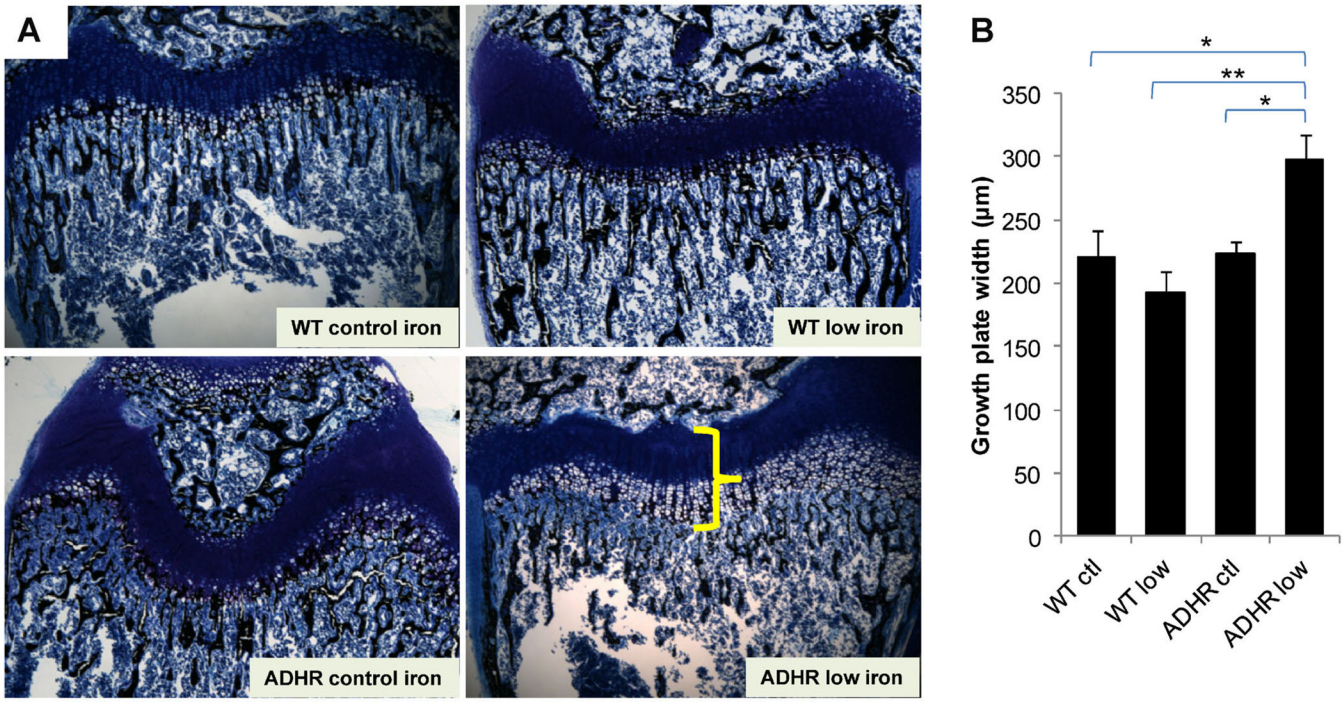

Fig. 4.

Distal femur histomorphometry. (*A*) Femur distal metaphysis sections were stained with McNeal/Tetrachrome and assessed using histomorphometry. The ADHR low-iron diet mice (lower right panel) had significantly widened growth plates characterized by an expanded zone of calcification (shown by yellow bracket) compared to WT control diet (upper left), WT low-iron diet (upper right panel), and ADHR mice receiving the control iron diet (lower left). (*B*) Quantification of the growth plate defect demonstrated significant increases in plate width for the ADHR low-iron group ("ADHR low") versus all other groups ($n = 4–5$/group: $^{**}p < 0.01$ versus WT low iron ("WT low"; $^{*}p < 0.05$ versus WT and ADHR control ("ctl") iron diet).

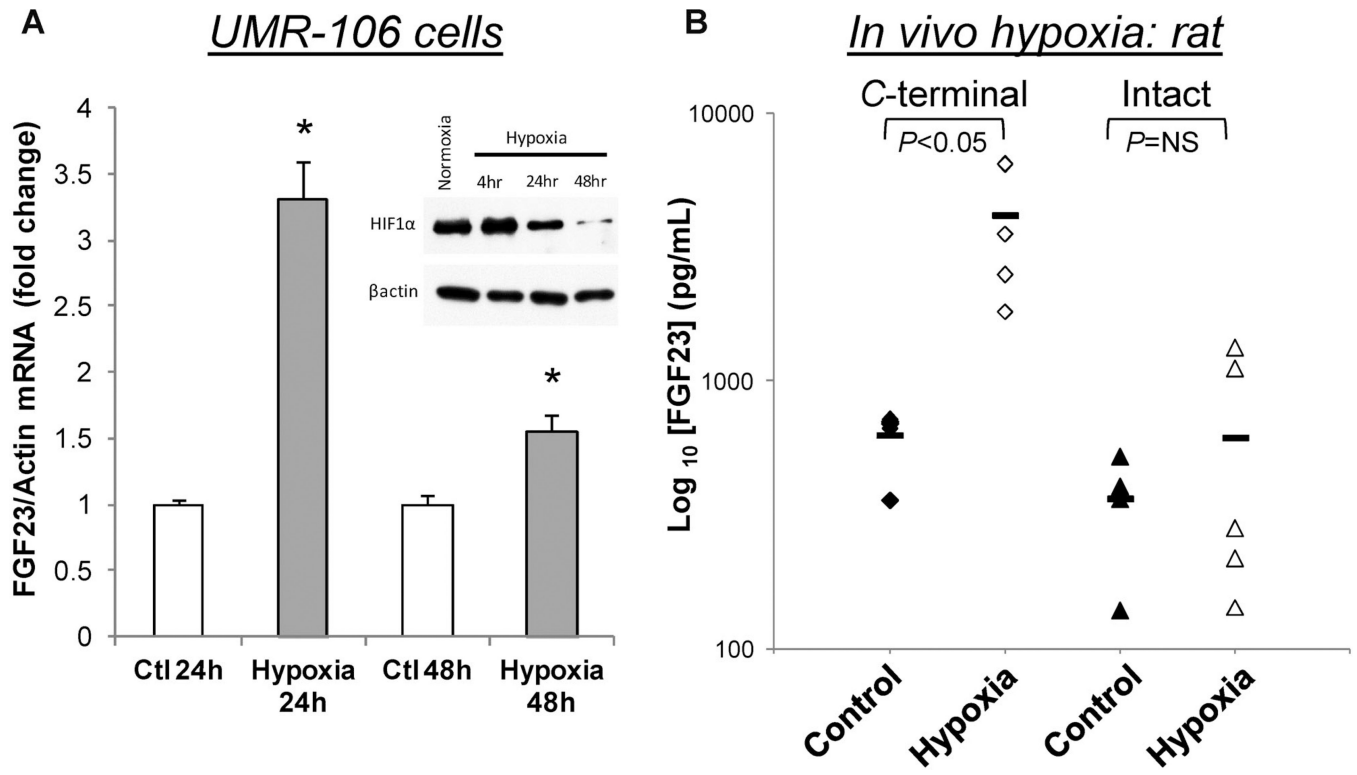

Fig. 5.

FGF23 stimulation by hypoxia in vitro and in vivo. (*A*) FGF23 mRNA was significantly elevated in UMR-106 cells cultured under hypoxic conditions for 24 to 48 hours. In parallel, immunoblots (chart inset) for HIF1α (upper panel) showed an increase at 4 hours, followed by reductions at 24 and 48 hours; the blot was stripped and β-actin was examined as the gel loading control (lower panel). (*B*) C-terminal, but not intact FGF23 was increased in rats (n = 5/group) housed under hypobaric hypoxia conditions for 2 weeks compared to rats housed under normoxia (*$p < 0.05$).

Table 1

Molecular and Biochemical Effects of Iron Repletion in ADHR Mice

	Serum Pi (mg/dL)	Intact FGF23 (pg/mL)	C-terminal FGF23 (pg/mL)	*FGF23* mRNA	*Cyp24a1* mRNA	*Cyp27b1* mRNA	*EPO* mRNA
ADHR: low iron	8.1 ± 0.18	741 ± 105	18,812 ± 1178	50.3 ± 5.3	10.8 ± 1.0	0.25 ± 0.1	70.9 ± 12.2
ADHR: control iron	13.8 ± 0.3	49.3 ± 5.2	375 ± 44	0.5 ± 0.2	1.3 ± 0.2	1.28 ± 0.2	1.2 ± 0.3
ADHR: replete iron	10.7 ± 0.2 *, **	61.5 ± 12 *	1,298 ± 205 *	3.6 ± 0.5 *	3.4 ± 0.9 *	0.22 ± 0.03 **	1.5 ± 0.4 *

All comparisons between ADHR control and low iron diet groups are at least $p < 0.05$.

ADHR = autosomal dominant hypophosphatemic rickets; FGF = fibroblast growth factor.

* $p < 0.01$ for replete iron versus ADHR mice provided continuous low iron diet.

** $p < 0.01$ for replete iron versus ADHR on control diet ($n \geq 10$).